

Received 29 September 2022; accepted 3 October 2022. Date of publication 6 October 2022; date of current version 12 October 2022.
The review of this article was arranged by Editor C.-M. Zetterling.

Digital Object Identifier 10.1109/JEDS.2022.3212432

Direct-Triggering LTT With Monolithic Structure

JINCHAO YIN¹, YUJIE BAI¹, KAI SHI¹, GUIPENG LIU¹, MING ZHOU², AND JIANHONG YANG¹

¹ School of Physical Science and Technology, Lanzhou University, Lanzhou 730000, China
² Jiangsu Mingxin Microelectronics Company Ltd., Hai'an 226634, China

CORRESPONDING AUTHOR: J. YANG (e-mail: yangjh@lzu.edu.cn)

ABSTRACT Light-triggered thyristor (LTT) has attracted considerable interest in power conversion and control systems because of its strong anti-interference ability and large power capacity. In this work, we propose a monolithic LTT that can be light-triggered directly without an amplifying gate (AG) design, to improve the device reliability and operating speed. The cathode structure is redesigned into an interdigitated structure with a relatively large light-incident area. The cathode shorts are rearranged to balance the trigger intensity and the light incident depth, so as to ensure optimal dV/dt capability. Devices are fabricated and adequate performances are obtained, verifying the feasibility of our design.

INDEX TERMS Light-triggered thyristor, monolithic, directly trigger, cathode structure, cathode short, dV/dt capability.

I. INTRODUCTION

As important power devices, thyristors have superior power handling capability and are widely used in power conversion and control in AC power circuits [1]. The control signal is electrically applied to the gate in conventional thyristors to initiate the turn-on process [2]. To obtain good anti-interference ability for reliable application in broad scenarios, light-triggered thyristors (LTTs) has been invented [3], [4]. In LTTs, the control signal is optically applied; a light source is used to generate electron-hole pairs in the active region, which yield a trigger current to turn on the device [5], [6], [7], [8].

LTTs are meant to be triggered using an optical signal instead of an electrical signal [9], [10], [11], [12], [13], [14], [15], [16]. However, most LTTs are each composed of two parts, one of which is of low power and the other is of high power, and the two parts are triggered one-by-one in a cascade manner: only after the low-power part is optically triggered ON, is the high-power part electrically triggered into ON state [17], [18], [19], [20], [21]. Such cascade triggering inherently deteriorates the turn-on process as a whole [22], [23], [24], [25], [26].

In this work, monolithic LTTs were designed and fabricated: the device was composed only one active part and could be triggered directly by a light signal as a whole.

The device structure and cathode topology were optimized compromisingly to obtain the adequate balance between light-control capability, electrical characteristics, and power handling capacity. The thickness of the base region, as well as its doping concentration, was designed to ensure maximum absorption of the incident light while ensuring sufficient forward blocking ability. The cathode topology, where the cathode shorts, the cathode contacts, and the transparent windows for the incident light were placed, was designed with an interdigitated pattern to allow enough light incident area while achieving the required dV/dt capacity.

II. DEVICE DESIGN AND FABRICATION

Fig. 1 (a) and Fig. 1 (b) compare the cascade-triggering and direct-triggering LTT structures. The cascade-triggering device, Fig. 1 (a), requires three amplifying gates (AGs), which are used to trigger one by one, thus delaying the turn-on process and complicating the fabrication process [10], [27], [28], [29]. In contrast, in the direct triggering device, as shown in Fig. 1 (b), the light source and the thyristor die are integrated into one package, and thus can be triggered directly without using multiple amplifying gates. The thickness of the N^+ cathode region is about 10 μm , where the doping concentration is $1 \times 10^{18} \text{ cm}^{-3}$. The thickness of the P-type base region is about 40 μm , where the doping concentration is $2 \times 10^{15} \text{ cm}^{-3}$. The doping

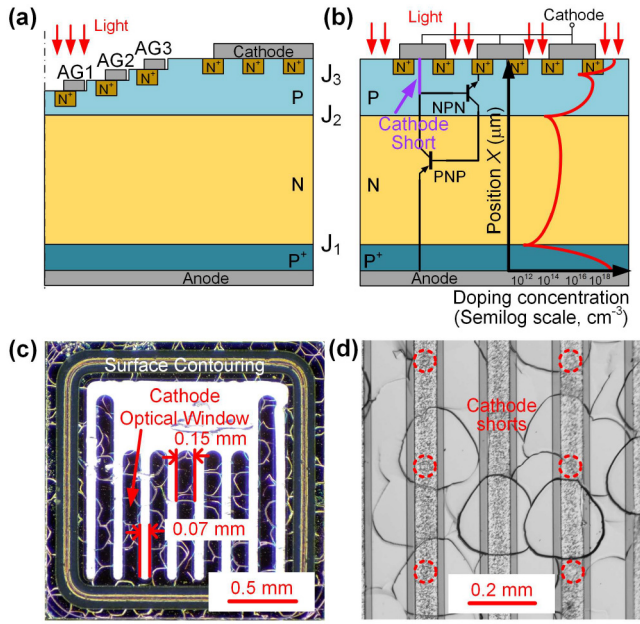


FIGURE 1. (a) The cross-section of cascade structure LTT; (b) the cross-section of monolithic LTT, the red curve shows the doping concentration distribution; (c) top-view of the fabricated monolithic LTT with key structural parameters; (d) local enlarged view of the fabricated monolithic LTT, in which the red circle represents the cathode shorts. The irregular bubble-like patterns in (c) and (d) are the shallow pits left by the etching of the silicon wafer.

concentration of the P-type region determines the critical breakdown electric field of the device, while the thickness affects the optical triggering sensitivity and blocking voltage of the device. The thickness of the N substrate is about 220 μm , and the doping concentration is $1 \times 10^{14} \text{ cm}^{-3}$. The thickness of the anode p region is about 10 μm , and the doping concentration of which is $1 \times 10^{19} \text{ cm}^{-3}$. This structure enables direct triggering instead of cascade triggering, thus improving the reliability and running speed of the device.

The device was fabricated with a 4-inch silicon wafer, and the finished die was $2.1 \times 2.1 \text{ mm}$ in size. Fig. 1 (c) shows the top view of the fabricated monolithic LTT, where the substrate uses a chemically corroded silicon wafer. As can be seen, the cathode is an interdigitated structure rather than a conventional large-area metal layer. The light incident windows were opened in the cathode metal layer, and the area of the windows accounted for nearly 50% of the total surface area of the device. This design eliminated the complex fiber coupling structure, and the laser could directly irradiate the surface of the device. It also allowed the utmost usage of the light signal, such that the device could be triggered using a much lower intensity of light. Besides, this cathode structure made a better trade-off between the light intensity and the light incident depth. The annular ring surrounding the active region in Fig. 1 (c) was a surface field terminating trench, which was filled with semi-insulating polycrystalline silicon (SIPOS) to improve the blocking performance. Under the cathode metal layer,

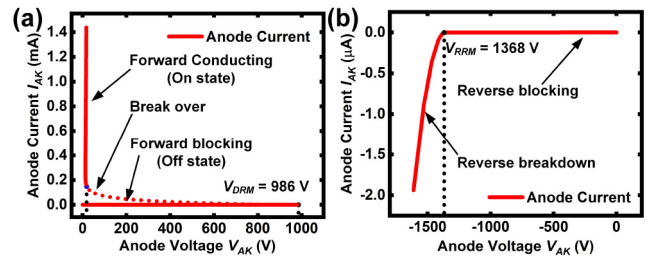


FIGURE 2. The output characteristics of the fabricated monolithic LTT: (a) forward output characteristics, and (b) reverse output characteristics.

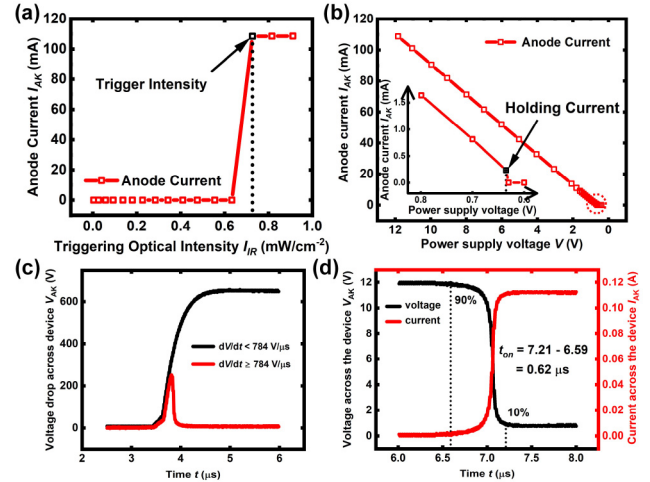


FIGURE 3. The on-state characteristics and switching characteristics of the fabricated monolithic LTT. (a) The typical light-triggering process; (b) The typical LTT holding current, where the inset shows the close-up of the turning point; (c) The voltage transient waveform under different dV/dt conditions; (d) The voltage and current transients of the LTT in the turn-on process.

there were specially designed cathode shorts to improve the dV/dt capability, as shown in Fig. 1 (d).

III. RESULTS AND DISCUSSION

The measurements of device characteristics were conducted strictly complying with the standards of the International Electrotechnical Commission (IEC 60747-6: 2016 Semiconductor devices - Part 6: Discrete devices - Thyristors). All measurements were carried out in the dark-room at room temperature (about 300 K). The triggering light used for the measurement was a popular laser with 940 nm output wavelength, and the optical intensity could be changed by adjusting the driving current.

The typical forward and reverse output characteristics of the LTT are shown in Fig. 2 (a) and Fig. 2 (b), respectively. It can be seen that the reverse blocking capability is slightly superior to the forward blocking capability. The forward repetitive peak voltage (V_{DRM}) reached 986 V, while the reverse repetitive peak voltage (V_{RRM}) reached 1368 V.

Fig. 3 (a) shows the light-triggering process. The circuit for the measurements complied with the common industrial test conditions, in which the laser current, and therefore the

optical intensity, could be adjusted to trigger the LTT. It can be seen from Fig. 3 (a) that when the optical intensity was below 0.7 mW/cm^2 , the current in the main circuit always remained close to 0, and the LTT was in a forward blocking state. When the optical intensity reached 0.73 mW/cm^2 , the current in the circuit increased abruptly, indicating that the device was turned on. The on-state voltage drop was about 1.0 V at 110 mA.

The measurement circuit for the holding current was the same as for the former process. After the device was turned on by the light trigger, the control circuit was disconnected, the main circuit was maintained in the on state, and the holding current was measured. Fig. 3 (b) shows the measurement results of a typical LTT holding current, where the inset displays the close-up of the turning point. As shown in Fig. 3 (b), when the voltage across the LTT in the main circuit continued to decrease, the current in the main circuit also linearly decreased, because the load used in the main circuit was resistive. When the current in the main circuit was below 0.235 mA, the current experienced a cliff-like drop to 0, which indicated that the LTT changed from a forward conducting state to a forward blocking state. Therefore, the holding current (I_H) of this device was 0.235 mA.

Fig. 3 (c) shows the measurement of dV/dt capability, where the voltage transient waveform under different dV/dt conditions are presented. dV/dt means the critical rate of rise of off-state voltage. The device exhibited a dV/dt capability of $784 \text{ V}/\mu\text{s}$ for the rising anode-cathode voltage from 0 V to 657 V ($2/3$ of the V_{DRM}). It had been observed that the device remained in OFF state as long as the dV/dt was smaller than $784 \text{ V}/\mu\text{s}$. In other words, it was the cathode shorts (as shown in Fig. 1 (d)) that allowed the device to avoid unexpected dV/dt triggering during the blocking operation by reducing the current gain of the NPN transistors in the thyristor.

As for the light triggering process, Fig. 3 (d) shows the voltage and current transients of the LTT in the turn-on process. The light-triggering signal initialized the turn-on process, and the turn-on time (t_{on}) of the LTT was determined to be $0.62 \mu\text{s}$. During this process, the voltage across the LTT decreases steeply from 12 V to 0.8 V while the voltage drop in the load increase from 0 V to 11.2 V, indicating that the LTT was turned on effectively.

Fig. 4 shows the comparison of the main parameters of this device with previously reported results. All the referenced devices have a cascade triggering mechanism with amplifying gates [30], [31], [32], but have almost the same die size and specifications as this work. As shown in Fig. 4, the forward repetitive peak voltage (V_{DRM}), the reverse repetitive peak voltage (V_{RRM}), and the dV/dt rating of this work are higher than the referenced results, while the trigger intensity, holding current, and turn-on time are less than those results. The overall performance of this work supports the rationality and feasibility of the design scheme for direct-triggering monolithic structure LTT.

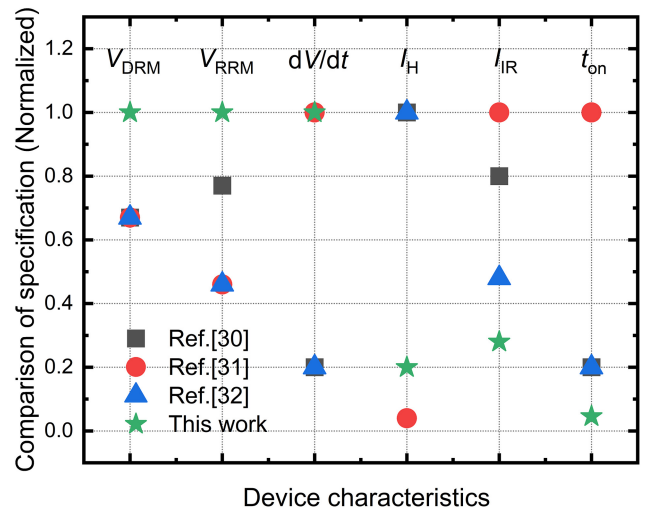


FIGURE 4. Comparison of this work with previously reported results.

IV. CONCLUSION

In summary, we proposed and fabricated an optimized monolithic and direct-triggering structural LTT. We demonstrated the feasibility of monolithic LTTs without using multiple amplifying gates. The rationality of the device design was verified by experiment results. As expected, we achieved the forward repetitive peak voltage of 986 V, the reverse repetitive peak voltage of 1368 V, and the dV/dt capability of $784 \text{ V}/\mu\text{s}$. The minimum optical trigger intensity needed only 0.73 mW/cm^2 , and the holding current was as low as 0.235 mA. More importantly, the turn-on time was decreased to $0.62 \mu\text{s}$ under normal operating conditions. Our results were encouraging for future high performance LTT design and potential applications.

REFERENCES

- [1] T. Adhikari, "Application of power electronics in the transmission of electrical energy," in *Proc. IEEE Region 10 Int. Conf. Global Connectivity Energy*, vol. 2, 1998, pp. 522–530, doi: [10.1109/TENCON.1998.798277](https://doi.org/10.1109/TENCON.1998.798277).
- [2] J. Rocabert, A. Luna, F. Blaabjerg, and P. Rodríguez, "Control of power converters in AC microgrids," *IEEE Trans. Power Electron.*, vol. 27, no. 11, pp. 4734–4749, Nov. 2012, doi: [10.1109/TPEL.2012.2199334](https://doi.org/10.1109/TPEL.2012.2199334).
- [3] S. Horiuchi, T. Horiuchi, and Y. Muraoka, "Development of VBO-free large capacity light-triggered thyristor valve," *IEEE Trans. Power Del.*, vol. 7, no. 1, pp. 276–280, Jan. 1992, doi: [10.1109/61.108918](https://doi.org/10.1109/61.108918).
- [4] J. Przybilla, R. Keller, U. Kellner, H.-J. Schulze, F.-J. Niedernostheide, and T. Peppel, "Direct light-triggered solid-state switches for pulsed power applications," in *Proc. 14th IEEE Int. Pulsed Power Conf. Dig. Tech. Papers*, vol. 1, Dallas, TX, USA, 2003, pp. 150–154, doi: [10.1109/PPC.2003.1277681](https://doi.org/10.1109/PPC.2003.1277681).
- [5] L. K. Tully, E. S. Fulkerson, D. A. Goerz, and R. D. Speer, "Evaluation of light-triggered thyristors for pulsed power applications," in *Proc. IEEE Int. Power Modulators High-Voltage Conf.*, 2008, pp. 1–4, doi: [10.1109/IPMC.2008.4743561](https://doi.org/10.1109/IPMC.2008.4743561).
- [6] J. Jensen and W. Merz, "Light triggered thyristor crowbar for klystron protection application," in *Proc. Particle Accelerator Conf.*, vol. 2, 2003, pp. 749–751, doi: [10.1109/PAC.2003.1289465](https://doi.org/10.1109/PAC.2003.1289465).
- [7] J. Holweg, H. P. Lips, B. Q. Tu, M. Uder, P. Baoshu, and Z. Yeguangu, "Modern HVDC thyristor valves for China's electric power system," in *Proc. Int. Conf. Power Syst. Technol.*, vol. 1, 2002, pp. 520–527, doi: [10.1109/ICPST.2002.1053597](https://doi.org/10.1109/ICPST.2002.1053597).

- [8] S. Kobayashi, T. Takahashi, S. Tanabe, T. Yoshino, T. Horiuchi, and T. Senda, "Performance of high voltage light-triggered thyristor valve," *IEEE Trans. Power App. Syst.*, vol. PAS-102, no. 8, pp. 2784–2792, Aug. 1983, doi: [10.1109/TPAS.1983.317961](https://doi.org/10.1109/TPAS.1983.317961).
- [9] T. H. G. G. Weise, B. Schuenemann, R. Keller, and J. Pzybilla, "Performance spectrum of optical triggered thyristor switches for electric weapon system," in *Proc. 12th Symp. Electromagnetic Launch Technol.*, 2004, pp. 252–254, doi: [10.1109/ELT.2004.1398084](https://doi.org/10.1109/ELT.2004.1398084).
- [10] W. Wang, X. Yan, J. Xiong, G. Du, and Y. Wang, "Study of driving characteristics of laser diodes used for triggering light-triggered thyristors (LTT)," in *Proc. IEEE Int. Conf. High Voltage Eng. Appl. (ICHVE)*, 2016, pp. 1–5, doi: [10.1109/ICHVE.2016.7800751](https://doi.org/10.1109/ICHVE.2016.7800751).
- [11] J. Yin, K. Shi, Y. Bai, L. Gu, M. Zhou, and Y. Jianhong, "Design and fabrication of monolithic light triggered thyristor," in *Proc. IEEE 16th Conf. Ind. Electron. Appl. (ICIEA)*, 2021, pp. 952–955, doi: [10.1109/ICIEA51954.2021.9516059](https://doi.org/10.1109/ICIEA51954.2021.9516059).
- [12] H. Nakao, Y. Nakagoshi, M. Hatano, and H. Miyata, "Test of a LTT thyristor valve for next generation 500 kV HVDC transmission system," in *Proc. IEEE Power Eng. Soc. Winter Meeting Conf.*, vol. 4, 2000, pp. 2932–2936, doi: [10.1109/PESW.2000.847351](https://doi.org/10.1109/PESW.2000.847351).
- [13] N. Holonyak, "The silicon p-n-p-n switch and controlled rectifier (thyristor)," *IEEE Trans. Power Electron.*, vol. 16, no. 1, pp. 8–16, Jan. 2001, doi: [10.1109/63.903984](https://doi.org/10.1109/63.903984).
- [14] S. C. Gao, T. Zhao, and D. Liu, "Development of 3125A/7600V light triggered thyristor," *Value Eng.*, vol. 33, no. 1, pp. 53–55, Jan. 2014, doi: [10.14018/j.cnki.cn13-1085/n.2014.01.145](https://doi.org/10.14018/j.cnki.cn13-1085/n.2014.01.145).
- [15] R. L. Cassel, "A 95 kV klystron power supply crowbar using light triggered SCR," in *Proc. 26th Conf. Record Int. Power Modulator Symp. High-Voltage Workshop*, 2004, pp. 478–480, doi: [10.1109/MODSYM.2004.1433617](https://doi.org/10.1109/MODSYM.2004.1433617).
- [16] A. Griffin, "Advances in photon triggered thyristors for high current applications," in *Proc. 27th Int. Power Modulator Symp.*, 2006, pp. 248–251, doi: [10.1109/MODSYM.2006.365229](https://doi.org/10.1109/MODSYM.2006.365229).
- [17] T. Wikström, B. Ødegård, and R. Baumann, "An 8.5kV sacrificial bypass thyristor with unprecedented rupture resilience," in *Proc. 31st Int. Symp. Power Semicond. Devices ICs*, Shanghai, China, 2019, pp. 491–494, doi: [10.1109/ISPSD.2019.8757563](https://doi.org/10.1109/ISPSD.2019.8757563).
- [18] G. Toulon, A. Bourennane, and K. Isoird, "Analysis and optimization of a thyristor structure using backside Schottky contacts suited for the high temperature," *IEEE Trans. Electron Devices*, vol. 60, no. 11, pp. 3814–3820, Nov. 2013, doi: [10.1109/TED.2013.2280554](https://doi.org/10.1109/TED.2013.2280554).
- [19] J. Przybilla, R. Keller, U. Kellner, C. Schneider, H. J. Schulze, and F. J. Niedernostheide, "Applications for direct light triggered thyristors with integrated protection functions," in *Proc. Int. Conf. Power Syst. Technol.*, vol. 2, Kunming, China, 2002, pp. 1029–1033, doi: [10.1109/ICPST.2002.1047556](https://doi.org/10.1109/ICPST.2002.1047556).
- [20] A. Mojab and S. K. Mazumder, "Design and characterization of high-current optical Darlington transistor for pulsed-power applications," *IEEE Trans. Electron Devices*, vol. 64, no. 3, pp. 769–778, Mar. 2017, doi: [10.1109/TED.2016.2635632](https://doi.org/10.1109/TED.2016.2635632).
- [21] A. Meyer, A. Mojab, and S. K. Mazumder, "Evaluation of first 10-kv optical ETO thyristor operating without any low-voltage control bias," in *Proc. 4th IEEE Int. Symp. Power Electron. Distrib. Gener. Syst.*, 2013, pp. 1–5, doi: [10.1109/PEDG.2013.6785592](https://doi.org/10.1109/PEDG.2013.6785592).
- [22] H. D. Sanders, S. C. Glidden, and D. M. Warnow, "Laser pumping of 5kV silicon thyristors for fast high current rise-times," in *Proc. IEEE Pulsed Power Conf.*, 2011, pp. 794–796, doi: [10.1109/PPC.2011.6191514](https://doi.org/10.1109/PPC.2011.6191514).
- [23] F. Niedernostheide, H. Schulze, J. Dorn, U. Kellner-Werdehausen, and D. Westerholt, "Light-triggered thyristors with integrated protection functions," in *Proc. 12th Int. Symp. Power Semicond. Devices ICs*, 2000, pp. 267–270, doi: [10.1109/ISPSD.2000.856822](https://doi.org/10.1109/ISPSD.2000.856822).
- [24] P. A. Mawby, and M. S. Towers, "Modelling of self-protected light-triggered thyristors," *IEE Proc. Circuits, Devices Syst.*, vol. 148, no. 2, pp. 55–63, 2001, doi: [10.1049/ip-cds:20010250](https://doi.org/10.1049/ip-cds:20010250).
- [25] H. Riazmontazer, A. Mojab, A. Rahnamaee, S. Mehrnami, S. K. Mazumder, and M. Zefran, "New single-bias all-optical ETO configuration for a 15 kV-100A SiC thyristor eliminating the turn-on leakage current," in *Proc. IEEE Appl. Power Electron. Conf. Expo.*, 2015, pp. 1250–1255, doi: [10.1109/APEC.2015.7104507](https://doi.org/10.1109/APEC.2015.7104507).
- [26] S. Katoh, S. Yamazumi, A. Watanabe, and K. Amemiya, "Overvoltage self-protection structure of a light-triggered thyristor," *IEEE Trans. Electron Devices*, vol. 48, no. 4, pp. 789–793, Apr. 2001, doi: [10.1109/16.915727](https://doi.org/10.1109/16.915727).
- [27] E. K. Chukaluri, D. Silber, U. Kellner-Werdehausen, C. Schneider, F. J. Niedernostheide, and H. J. Schulze, "Recent developments of high-voltage light-triggered thyristors," in *Proc. IEEE 36th Power Electron. Specialists Conf.*, 2005, pp. 2049–2052, doi: [10.1109/PESC.2005.1581914](https://doi.org/10.1109/PESC.2005.1581914).
- [28] B. G. Streetman and S. Banerjee, *Solid State Electronic Devices*, 7th ed. Hoboken, NJ, USA: Prentice Hall, 2013, pp. 534–535.
- [29] B. J. Baliga, *Fundamentals of Power Semiconductor Devices*, Power Semicond. Research Center, North Carolina State Univ., Raleigh, NC, USA, 2008, pp. 637–639.
- [30] "Industrial Devices." Panasonic Corporation. Accessed: Sep. 22, 2020. [Online]. Available: https://www3.panasonic.biz/ac/e/search_num/index.jsp?c=detail&part_no=AQH2223
- [31] "Phototriac Coupler." Sharp devices Europe. Accessed: Apr. 19, 2017. [Online]. Available: <https://www.sharpsde.com/products/optoelectronic-components/model/pc3sd12ntzah#productview>
- [32] "Optocoupler, power phototriac." Vishay Intertechnology the United States of America. Accessed: Mar. 18, 2021. [Online]. Available: <https://www.vishay.com/product?docid=81166>.